

Effect of Interface on Mechanical Properties of Ti/Al/Mg/Al/Ti Laminated Composites

Miao Cao^a , Cui-ju Wang^a, Kun-kun Deng^{a,b,*}, Kai-bo Nie^a, Wei Liang^{a,b}, Yu-cheng Wu^{a,b}

^aTaiyuan University of Technology, College of Materials Science and Engineering, Shanxi Key laboratory of advanced magnesium-based materials, Taiyuan 030024, PR China

^bTaiyuan University of Technology, Ministry of Education, Key Laboratory of Interface Science and Engineering in Advanced Materials, Taiyuan 030024, China

Received: November 26, 2019; Revised: January 20, 2020; Accepted: January 29, 2020

Ti/Al/Mg/Al/Ti laminated composites were fabricated via hot-pressing at 350 °C, 400 °C and 450 °C successfully. The influences of interface morphology, diffusion zone, constraint effect on the mechanical properties were investigated. At Ti/Al interface, intermetallic compounds aren't found. Whereas, they form at Al/Mg interface. With the increasing temperature, the bonding strength of Al/Mg interface doesn't change linearly, and the maximum strength is obtained at 400 °C because of intermetallic compounds with appropriate thickness. With the increase of temperature, the hardness at both Ti/Al and Al/Mg interfaces increases owing to the solid solution and the intermetallic phases. Also, the ultimate tensile strength of LMCs increases with sacrificing the fracture elongation. The rule of mixture is used to predict the theoretical strength. It is found that the theoretical values are less than the measured, and the reasons may relate to interfaces in Ti/Al/Mg/Al/Ti laminated composites.

Keywords: Hot-pressing, Interface, Bonding strength, Hardness, The rule of mixture

1. Introduction

Laminated composites, which possess excellent ductility, strength and density, have drawn growing attention^{1,2}. And plenty of metals have been adopted to prepare metal laminated composites. Mg and its alloys have been widely used due to their high specific strength, damping performance and low density. However, the inferior corrosion resistance, stiffness and abrasion resistance severely confine their development³. Ti and its alloys are preferred where excellent specific strength, fracture toughness, temperature resistance and corrosion resistance are required⁴. Coating Ti layer on the surface of Mg not only overcomes their shortcomings but also takes advantage of dissimilar metals. However, almost no solid solubility or chemical reaction between Ti and Mg alloys raises a challenge to metallurgical bonding. Consequently, an intermediate layer should be added at Ti/Mg interface to facilitate atomic diffusion or reaction. In reality, the in-depth studies had been done on Mg/Al⁵ and Ti/Al⁶ composites in previous works. Accordingly, it is feasible to fabricate Ti/Al/Mg/Al/Ti laminated composites by using Al as a connection layer between Ti and Mg sheets⁷.

Currently, solid-solid synthesis has been widely used because of fewer pores, oxidation inclusions and higher bonding strength than traditional fusion techniques. Solid-solid synthesis includes rolling⁸, hot-pressing⁹, explosive welding¹⁰, extrusion^{11,12} and two or more of them (such as explosive welding and rolling⁵, hot-pressing and rolling¹³ and so on). For instance, Zhang et al.⁸ manufactured Al/Cu/Ti/Cu/Al laminated composites via cold-rolling, exploring the fracture mechanism. Qin et al.⁶ applied hot-pressing method to fabricating Ti/Al composites and examined the formabilities.

Saravanan et al.¹⁴ researched the interface properties of Al/Cu composites prepared by explosive welding. In the study carried out by Chen et al.¹⁵, the Al/Mg/Al composites were prepared by extruding, and the effects of temperature on interface and microstructure were investigated. Zhang et al.¹⁶ designed ZW31/PMMCs composites by extrusion followed by rolling to solve the rolling problem of micron particle reinforced magnesium matrix composites. Furthermore, explosive welding and rolling were used by Fronczek and Chulist¹⁷ to fabricate Al1050/AZ31/Al1050 composites, and the evolution rule of interface structure and intermetallic phases was probed. Assari and Eghbali¹⁸ researched the structure sequence of Ti-Al multi-laminated composite produced by hot-pressing and rolling. Among the methods above, hot-pressing is a promising technique employed in the fabrication of Ti/Al/Mg laminated composites for the advantages of cheap manufacturing and easy operation, and the metallurgical bonding can be achieved on the basis of element diffusion at high temperature. Meanwhile, the stable and excellent mechanical properties can also be realized in this way.

So far, plentiful works on Ti/Al composites have been done, such as layer thickness ratio¹⁹, reaction kinetics of phases at the interface²⁰, annealing process²¹, deformation mechanism of monolithic metal²² and formability²³. And the researches on Mg/Al composites mainly focused on the preparation technology²⁴, bonding quality²⁵, precipitated phases¹¹, formability²⁶ and so on. However, the investigations on Ti/Al/Mg/Al/Ti laminated composites are rare, especially the comprehensive influences of Ti/Al and Al/Mg interfaces on the mechanical properties of Ti/Al/Mg/Al/Ti laminated composites still require to be enriched.

*e-mail: dengkunkun@tyut.edu.cn

In present work, the Al layer located between Ti layer and Mg layer in order to achieve better interface bonding, and the hot-pressing was adopted to prepare Ti/Al/Mg/Al/Ti laminated composites. The influence of hot-pressing temperatures on the interface structure and the mechanical properties was discussed. In particular, the applicability of the rule of mixture (ROM) on evaluating strength was checked, and the reasons for the gap between the measured values and the theoretical values were also analyzed for the purpose of better understanding on mechanical behavior of Ti/Al/Mg/Al/Ti laminated composites. The above research fruits, as a supplement in the field of laminated composites, are thought to provide guidance for the industrial production of Ti/Al/Mg/Al/Ti laminated composites.

2. Experimental Procedures

2.1 Materials and laminate processing

Commercial TA1 pure Ti, 2024 Al and AZ31B Mg are chosen as the component layers of Ti/Al/Mg/Al/Ti laminated composites. The TA1, 2024 Al and AZ31B plates with original thickness of 0.3 mm, 0.5 mm and 1 mm, respectively, all are cut into the size of 100 mm × 60 mm (the rolling direction (RD) × the transverse direction (TD)). The initial grain sizes of TA1 and AZ31B are ~7.69 μm and ~3.83 μm, respectively, as illustrated in Figure 1. For convenience, LMCs, Ti, Al and Mg are used to represent Ti/Al/Mg/Al/Ti laminated composites, TA1, 2024 Al and AZ31B Mg, respectively.

LMCs are fabricated by hot-pressing, and the preparation processes are illustrated in Figure 2. (i) The surfaces of Ti, Al and Mg are cleaned and roughened with a steel brush to

remove surface dirt and oxide layers. The following specific steps include ultrasonic cleaning and rapid drying. (ii) The above plates are stacked in the order of Ti/Al/Mg/Al/Ti along the same direction, then they are put into the hot-pressing mold. (iii) The preparation technology is explored firstly. Figure 3 shows the macro morphologies of LMCs fabricated at different pressures and temperatures. At 200 MPa, Ti and Al are not bonded at 300 °C, while Mg is crushed out of LMCs at 500 °C, as shown in Figure 3a, thus the suitable temperature is 400 °C. Once the temperature is set as 400 °C, the bonding of LMCs depends on the pressure. As presented in Figure 3b, the well-bonding between Ti and Al doesn't occur at 175MPa, and obvious cracks in Ti are visible at 225MPa, therefore only the pressure of 200MPa is a suitable one. Referring to the above results, the pressure of 200 MPa is adopted in present work. In order to reveal the effects of hot-pressing temperatures on the interface structure and mechanical properties of LMCs, the temperatures of 350°C, 400°C and 450°C are selected, and well-bonded LMCs are obtained at these temperatures. Detailed hot-pressing processes are demonstrated in Figure 3c.

2.2 Microstructure observation

Metallographic samples are fabricated by standard mechanical grinding and polishing, and the RD-ND planes are observed. LMCs are etched in Keller reagent (3ml HF + 2ml HNO₃ + 95ml H₂O) and 3.5% nitrate + 4% oxalic acid solution. The metallographic tests of Mg and Ti are carried out via optical microscope (OM). And US8010 Scanning Electron Microscope (SEM) equipped with an energy dispersive spectrometer (EDS) is adopted to achieve interfacial microstructure observation.

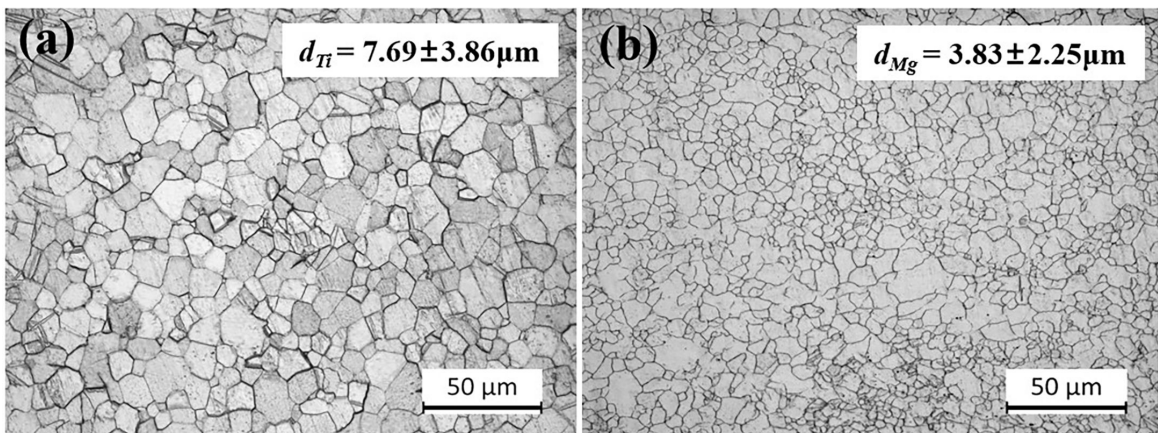


Figure 1. The metallographic structure of the original sheets of (a) TA1 and (b) AZ31B.

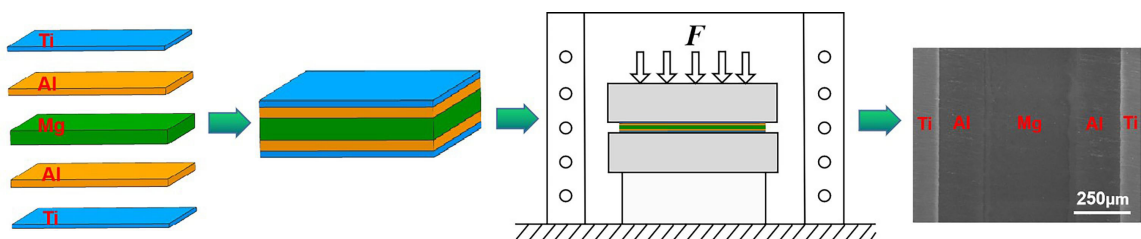


Figure 2. The schematic diagrams of fabricating Ti/Al/Mg/Al/Ti laminated composites.

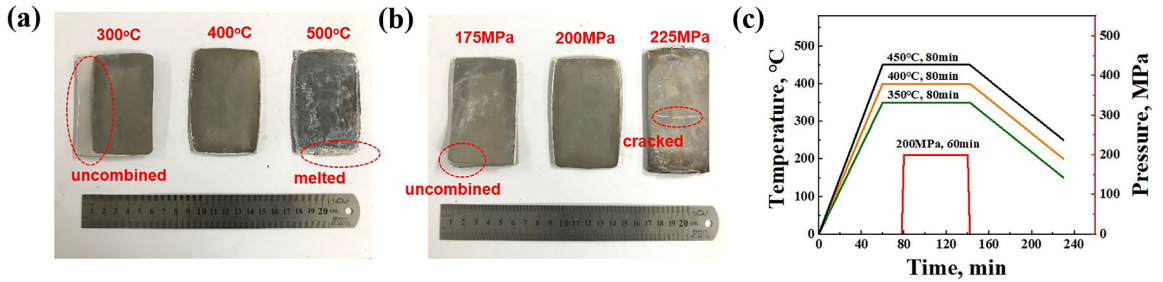


Figure 3. Exploration of (a) temperature at 200 MPa and (b) pressure at 400 °C during the preparation of LMCs, (c) the preparation technology of Ti/Al/Mg/Al/Ti LMCs.

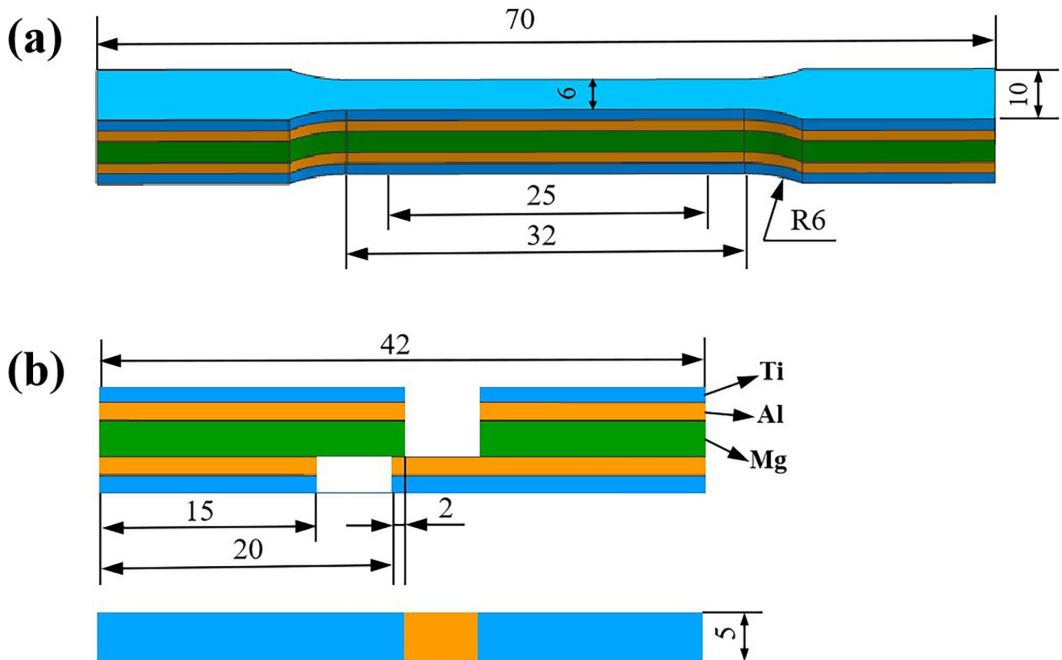


Figure 4. The schematic diagrams of specimens for (a) uniaxial tensile tests and (b) shear tests.

2.3 Mechanical properties test

The mechanical properties of LMCs and monolithic Ti, Al and Mg are measured using MTS (E45.105) electronic universal testing machine. And the size of tensile specimens is shown in Figure 4a. An extensometer with a gauge of 25 mm is applied to tensile specimens, and three specimens under each condition are tested at a constant crosshead speed of 1mm/ min.

The vickers hardness is measured with HV-1000 Micro Vickers Hardness Tester under a load of 100g for 15s.

The shear tests are performed to evaluate the interface bonding quality according to GB/T 6396-2008 standard. The specimens with an overlap joint size of 2×5 mm (RD×TD) are cut using wire electrical discharge machines, as shown in Figure 4b. The shear tests are conducted on MTS (E45.105) electronic universal testing machine with a speed of 0.5mm/min. The formula for calculating interface bonding strength is as follow: $P = F/S$, where F is tensile load and S represents bonding area.

3. Results and Discussion

3.1 Microstructure

Figure 5 presents the SEM images of Ti/Al interface. As shown in Figure 5a, well-bonded interfaces are obtained and no conspicuous voids or delamination can be observed. It is interesting that the morphologies of Ti/Al interfaces exhibit significant differences. At 350 °C, flat Ti/Al interface is observed, but it becomes rough at 400 °C and 450 °C. Which is attributed to the nonuniform deformation of adjacent metals with different plastic deformation ability. The appearance of rough interfaces is considered to be a signal of enhanced bonding strength¹⁹. Figure 5a shows the EDS line analysis results of Ti/Al interface at different temperatures, and the obvious diffusion layers indicate metallurgical bonding between Ti and Al. The width of diffusion layers are 1.0 μm, 1.5 μm and 2.1 μm at the temperatures of 350 °C, 400 °C and 450 °C, respectively. The higher the temperature is, the wider the diffusion layer is¹⁵. As illustrated in Figure 5b, EDS point

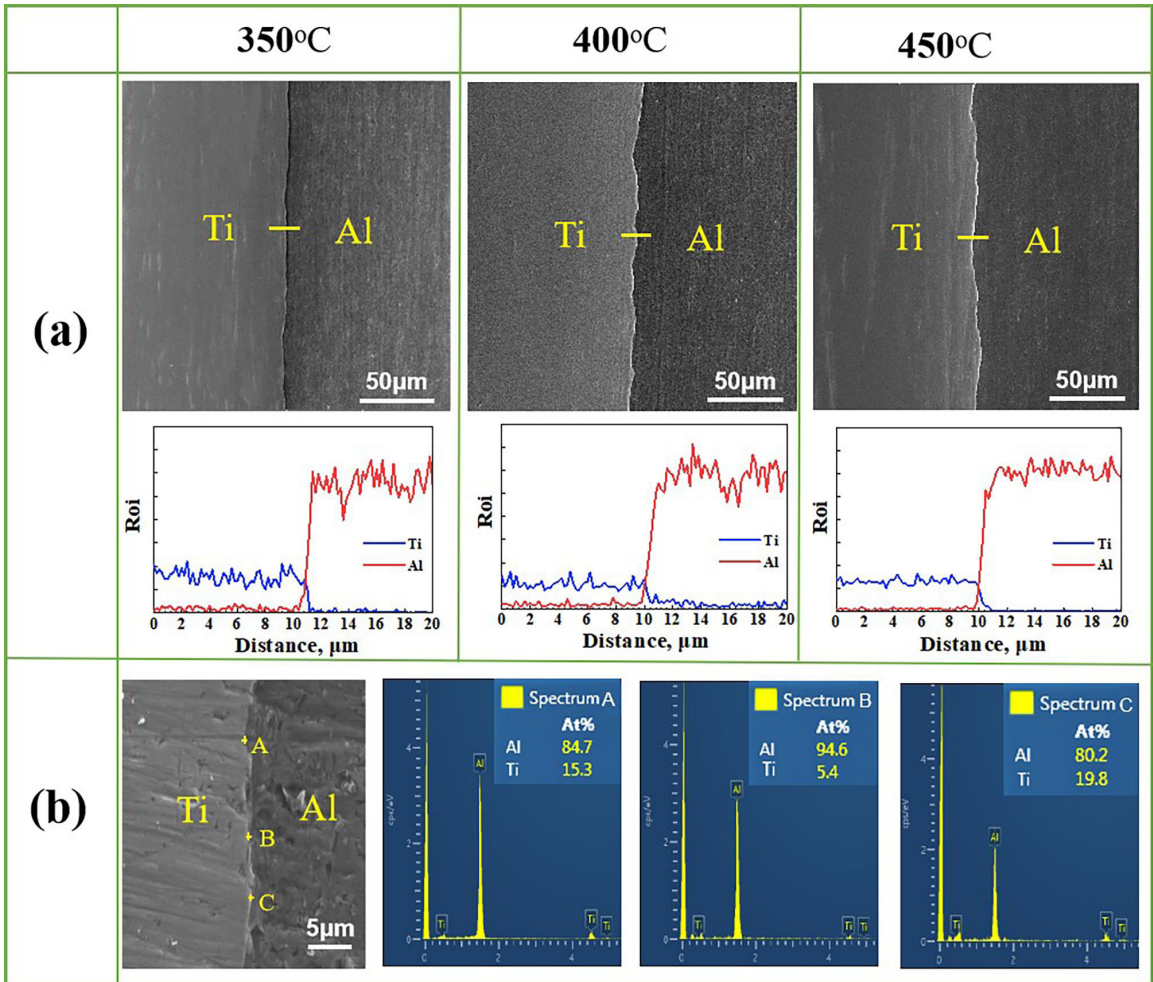


Figure 5. The SEM images of Ti/Al interface in LMCs: (a) the EDS line analysis at different temperatures, (b) the EDS point analysis at 450 °C.

analysis at Ti/Al interface is performed at 450 °C. Combining with the EDS line analysis results of no platform on the curves in Figure 5a, it can be concluded that intermetallic phases don't form at Ti/Al interface when hot-pressed at 450 °C. Due to the insufficient atomic diffusion at 350 °C and 400 °C, the same results can be obtained.

The SEM images of Al/Mg interface are given in Figure 6. As can be seen from Figure 6a, obvious intermetallic phases layers are found, and their thicknesses increase as the temperature increases. Also, two layers marked by yellow dotted line in Al/Mg interface can be identified. According to the EDS point analysis results of Figure 6c, Al_3Mg_2 phase near Al layer and $\text{Mg}_{17}\text{Al}_{12}$ phase near the Mg layer are found. Based on the Al-Mg phase diagram and the previous works^{26,27}, the same conclusion can also be achieved. The thicknesses of intermetallic phases layers at Al/Mg interface are $\sim 10.56 \mu\text{m}$, $\sim 25.12 \mu\text{m}$ and $\sim 38.40 \mu\text{m}$ at 350 °C, 400 °C and 450 °C, respectively. The EDS analysis results in Figure 6b also display a thickened diffusion region.

Both Ti/Al and Al/Mg interfaces are well-bonded displayed in Figure 5a and Figure 6a. The film theory²⁸ indicates two contacted surface layers (including oxide film

and contaminant film formed by brush scraping) break up and virgin metals are extruded through cracks under high temperatures and pressures. However, the adjacent sheets may not be bonded even if the virgin metals are exposed, unless the deformation is larger than a certain threshold²⁹. According to the energy barrier theory, the energy such as dispersing surface contaminants, extruding virgin metals, rearranging atoms to reconstruct grain boundary and activation energy are required for bonding metals. In present work, the rough surface is obtained by scratching with a steel brush during pretreatment. Thus the mechanical interlocking is achieved at the early stage of hot-pressing. And the pressure of 200 MPa applied to LMCs could overcome the energy barrier required for bonding metals. In an analysis of the changes of Ti/Al interface morphology, the differences on crystal structure and mechanical properties between Al and Ti must be considered. Pure Ti with HCP lattice below phase transition temperature (882 °C) possesses higher deformation resistance as compared with Al with FCC lattice. During deformation, shear occurs at the interface, which becomes much more drastic with the increasing temperature. Eventually strain localization generates near

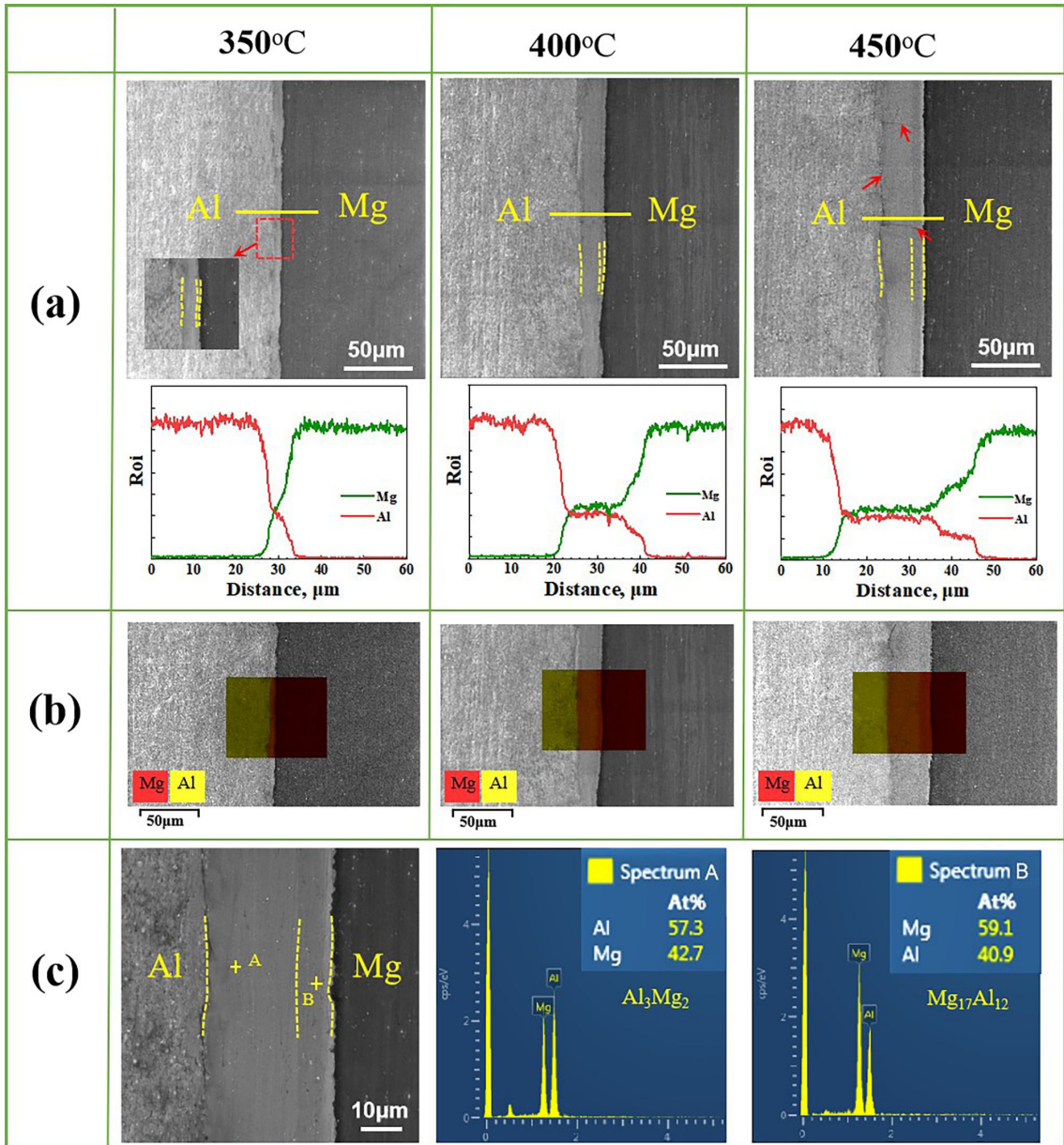


Figure 6. The SEM images of Al/Mg interface in LMCs: (a) the EDS line analysis and (b) the EDS map analysis at different temperatures, (c) the EDS point analysis at 450 °C.

Ti/Al interface, so that protrusion and retraction form along the interface²⁹. Furthermore, the difference of the thermal expansion coefficients between Ti and Al (Al is $18 \sim 24 \times 10^{-6}/K$, and Ti is $8.4 \sim 8.6 \times 10^{-6}/K$) may cause a thermal stress at the interface during the cooling after hot-pressing²¹. These may result in some elastic-plastic deformation near the interface and finally trigger uneven interface.

From the EDS analysis results of Ti/Al and Al/Mg interfaces in Figure 5a and Figure 6a, the diffusion layer thickens with the increase of temperature. Previous works had demonstrated that elements diffusion was promoted through three basic mechanisms: mechanically induced atomic displacement, pipe diffusion along dislocations and vacancy diffusion induced by plastic deformation³⁰. During

hot-pressing, a large number of dislocations and vacancies are induced by severe plastic deformation. However, it is hard for dislocations to move by carrying atoms under high pressure. While the concentration and the mobility of vacancies enhance with the increasing temperature. As a result, diffusion at the interface accelerates owing to the migration of vacancies.

It can be seen from the EDS point analysis results in Figure 5b that intermetallic phases don't form at Ti/Al interface. Ma et al.²⁸ and Xia et al.³¹ also didn't find intermetallic phases at Ti/Al peeling surface of rolled and explosive welded Ti/Al layered composites because of the shorter reaction time. While Du et al.³² detected $TiAl_3$ phase with a DO22 structure at Ti/Al interface fabricated

by vacuum hot-pressing and hot-rolled. Also, Yu et al.²¹ proved that $TiAl_3$ was the only phase that could form and grow at Ti/Al interface after annealing at 873 K for 6 h for as-rolled Al/Ti/Al. Based on above analysis, the nucleation and growth of phases depend on thermodynamic and kinetic conditions. At low temperatures, the nucleation is mainly related to atoms diffusion along grain boundaries. It is hard for Ti and Al atoms to diffuse massively in a short time due to insufficient atomic concentration and energy. Therefore, the formation of Ti-Al intermetallic phases is impossible.

As marked by the yellow dotted line in Figure 6c, the intermetallic phases layer can be seen clearly. According to Al-Mg binary phase diagram, the maximum concentration of Mg in Al and Al in Mg are 18.9 at % (at 450 °C) and 11.8 at % (at 437 °C), respectively. At the beginning of diffusion, diffusion between Mg atoms and Al atoms will form solid solution due to the driving force of concentration gradient. When the concentration is more than the maximum

equilibrium concentration, the Al_3Mg_2 and $Mg_{17}Al_{12}$ precipitate from supersaturated solid solution of Al (Mg) and Mg (Al), respectively. The similar results were also confirmed by Yang et al.'s investigation⁵. During the subsequent reaction process, a large number of intermetallic phases precipitate continuously, which accumulate and form a thin layer along the interface. After that, due to the concentration gradient between Mg/Al layer and new phases, the new phases grow in the direction perpendicular to the interface. Finally, a thick intermetallic phases layer forms.

Figure 7 demonstrates the OM images and grain sizes distribution of Ti and Mg in LMCs at different hot-pressing temperatures. The grain sizes of Ti are $\sim 7.01 \mu m$, $\sim 7.34 \mu m$ and $\sim 7.89 \mu m$ at 350 °C, 400 °C and 450 °C, respectively, only slight growth occurs. Considering that the melting point of pure Ti is 1668 °C, the Ti can be categorized as a warm-deformed structure at current temperatures. So the influence of temperature on grain size of Ti is not evident.

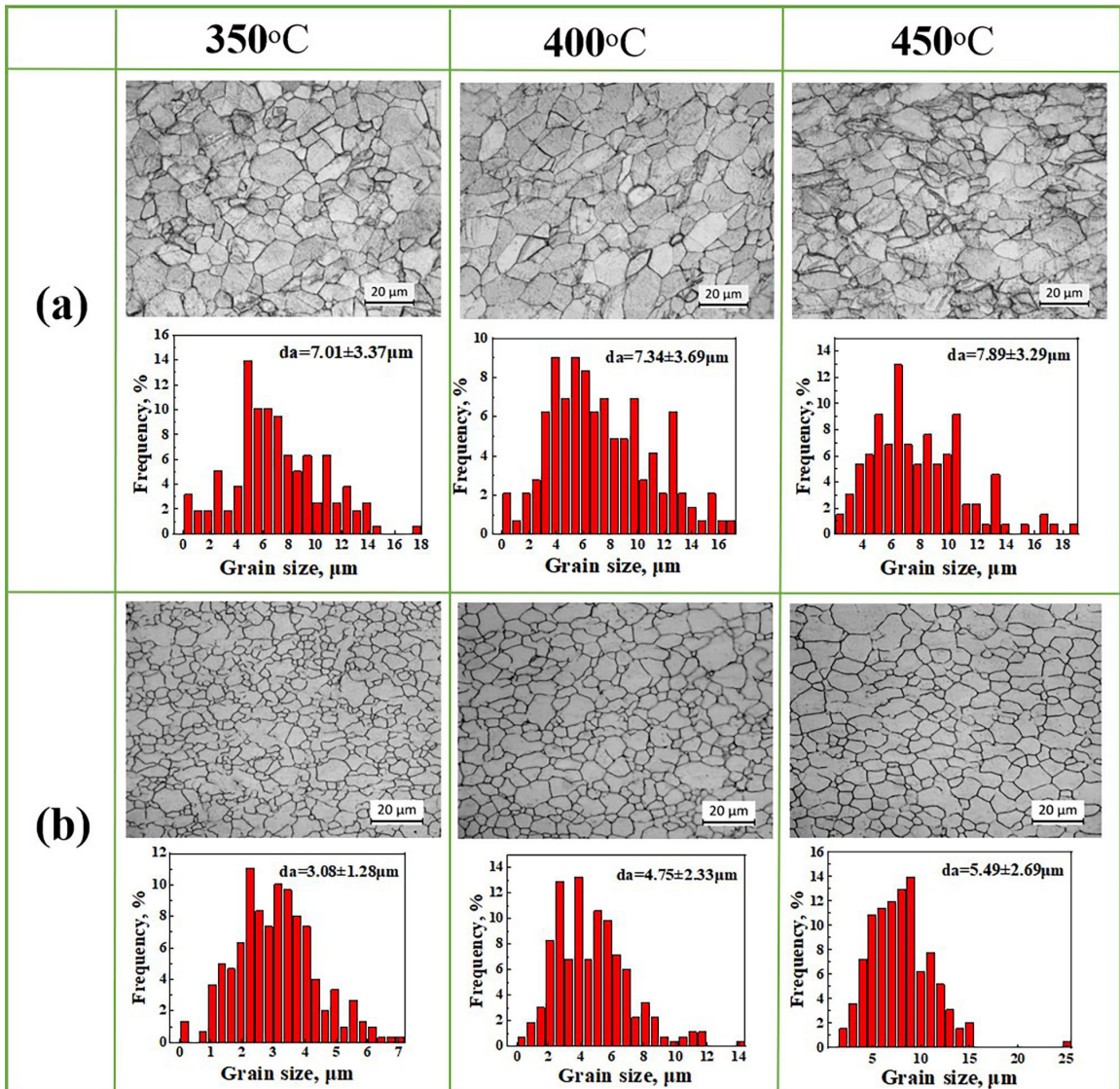


Figure 7. Metallographic structure and grain size distribution of (a) Ti and (b) Mg at different hot-pressing temperatures.

It is interesting that a small number of twins are observed in Ti at 450 °C. The twins may be associated with the strain distribution during hot-pressing¹⁴. The recrystallization occurs in Mg at various temperatures. The grain sizes of Mg are ~3.08 μm , ~4.75 μm and ~5.49 μm at 350 °C, 400 °C and 450 °C, respectively. At 350 °C, a host of equiaxial fine grains are found at grain boundaries, especially at trigeminal grain boundaries²⁵. With the increase of temperature, the migration rate of grain boundaries accelerates, the grain size reaches the maximum and the distribution becomes more uniform at 450 °C. As shown in Table 1, the deformation of LMCs increases with the increase of temperature. Moreover, at high temperature, the higher strain energy in LMCs also provides driving force for grains growth.

3.2 Bonding strength

Huang et al.³³ suggested that the high ductility of Ti-Al composites benefited from strong bonded interface, which not only reduced the strain localization of Ti layer, but also effectively relieved the stress concentration of Al layer. However, Launey et al.³⁴ stated that delamination occurred easily at weak bonded interface, which could effectively restrict the crack propagation via crack deflection and blunting, thus toughening was achieved. Therefore, it is indispensable to evaluate bonding strength. In present work, bonding strength is measured by shear tests. Figure 8. shows

variations of interface bonding strength for LMCs prepared at different hot-pressing temperatures.

From bonding strength-strain curves of Ti/Al interface in Figure 8a and variations of Ti/Al interface bonding strength in Figure 8c, it is observed that both bonding strength and fracture strain of Ti/Al interface increase continuously with the temperature increases. At 350 °C, 400 °C and 450 °C, Ti/Al interface bonding strength are 8.75 MPa, 25.8 MPa and 29.1 MPa, respectively. Especially from 350 °C to 400 °C, interface bonding strength increased by 195%. At 350 °C, at low strain, interface debonding occurs because of weak bonding. With the temperature increases, the strong interface leads to an enhanced constraint effect between Ti layer and Al layer, so fracture strain increases. The changes of Ti/Al interface bonding strength can be explained by the following aspects. From the perspective of deformation, with the temperature increases, the deformation of LMCs increases (as shown in Table 1), and the oxide layer and the dirt layer at the interface rupture, so more virgin metal is available in the contact surfaces for atom-to-atom bonding. Bouaziz et al.³⁵ also found that the higher strains can improve interface bonding. Moreover, the higher deformation can easily cause severe shear deformation at the interface, thereby rough interfaces are introduced. The rough interfaces increase the actual contact area between Ti and Al, and is conducive to improving bonding strength. From the perspective of

Table 1. The thickness of Ti, Al, Mg and Al/Mg intermetallic layers in LMCs after hot-pressing at different hot-pressing temperatures.

Temperature, °C	Type of layer	Thickness of layer, μm	Reduction of layer, %
350	Ti	257.75 \pm 2.78	14.08
	Al	394.57 \pm 2.43	21.09
	Mg	790.46 \pm 2.85	20.95
	Al/Mg intermetallic	10.56 \pm 1.94	/
	LMCs	2105.66	19.01
400	Ti	247.22 \pm 1.51	17.59
	Al	379.50 \pm 6.36	24.10
	Mg	780.01 \pm 1.25	22.20
	Al/Mg intermetallic	25.12 \pm 0.25	/
	LMCs	2056.57	20.90
450	Ti	228.97 \pm 3.73	23.68
	Al	336.99 \pm 2.81	32.60
	Mg	685.96 \pm 2.81	31.40
	Al/Mg intermetallic	38.40 \pm 1.54	/
	LMCs	1856.28	28.60

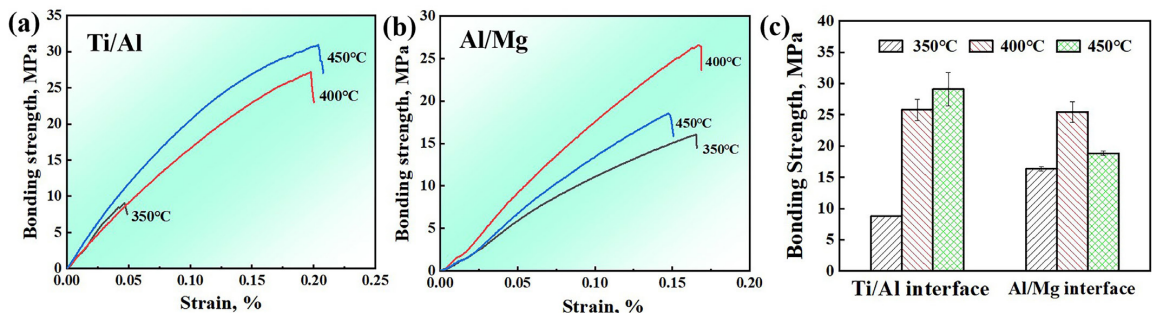


Figure 8. Variations of interface bonding strength for LMCs prepared at different hot-pressing temperatures: bonding strength-strain curves of (a) Ti/Al interfaces and (b) Al/Mg interfaces, (c) variations of bonding strength for Ti/Al and Al/Mg interfaces.

diffusion, with the temperature increases, the diffusion rate of Ti and Al atoms accelerates, and the diffusion layer thickens, which leads to enhanced metallurgical bonding²⁵. Furthermore, intermetallic compounds don't form at Ti/Al interface as shown in Figure 5b, so their adverse effects are unnecessary to consider.

Figure 8b and Figure 8c show bonding strength-strain curves of Al/Mg interface and variations of Al/Mg interface bonding strength, respectively. At 350 °C, 400 °C and 450 °C, Al/Mg interface bonding strength are 16.35 MPa, 25.45 MPa and 18.85 MPa, respectively. From 350 °C to 400 °C, interface bonding strength increases, while it reduces from 400 °C to 450 °C. The changes of fracture strain is consistent with bonding strength. Different from Ti/Al interface, the bonding quality of Al/Mg interface has close relationship with transition layer. The formation of intermetallic phases is a symbol of metallurgical bonding, while intermetallic phases layer with excessive thickness is negative for bonding quality¹¹. With the increase of temperature, intermetallic phases layer at Al/Mg interface thickens gradually³⁶. At 350 °C or 400 °C, intermetallic phases can be regarded as reinforced phases, thus bonding strength improves. However, intermetallic phases layer thickens transversely at 450 °C, which deteriorates the bonding strength of Al/Mg interface. Also quite a few microcracks can be seen in intermetallic phases layer, as shown by red arrows in Figure 6a. Hence, the bonding strength of Al/Mg interface

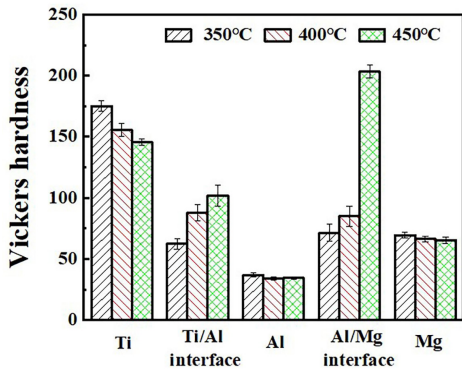


Figure 9. The micro-hardness values of Ti layer, Ti/Al interface, Al layer, Al/Mg interface and Mg layer in LMCs fabricated at different hot-pressing temperatures.

decreases as the temperature increased to 450 °C. Choi et al.²⁷ also confirmed that intermetallic phases layer with appropriate thickness had a positive effect on mechanical properties of Al-Mg welded joints.

3.3 Micro-hardness

Figure 9 exhibits the micro-hardness values of Ti layer, Ti/Al interface, Al layer, Al/Mg interface and Mg layer in LMCs. It indicates that the micro-hardness of Ti layer, Al layer and Mg layer reduces with the increase of temperature. As described in Figure 7, the grain sizes increase gradually with the increase of temperature, and coarse grains lead to low hardness values of monolithic sheet according to Hall-Petch relationship. However, the hardness increases with the rise of temperature at both Ti/Al and Al/Mg interfaces. Especially, the hardness of Al/Mg interface soars to 203.18HV at 450 °C. For Ti/Al interface, solution strengthening plays a vital role. Lyu et al.²⁹ also reported that the hardness of Ti layer increased owing to the increase of solid solubility of Al in Ti. As to Al/Mg interface, $Mg_{17}Al_{12}$ and Al_3Mg_2 form at 450 °C. Chang et al.³⁷ and Yang et al.³⁸ had found that the $Mg_{17}Al_{12}$ and Al_3Mg_2 possessed higher elastic modulus and nano-hardness than the matrix. Thus, intermetallic phases are responsible for the high micro-hardness at Al/Mg interface.

3.4 Tensile properties

The thickness of LMCs decreases in the normal direction (ND), and the length increases along RD as well as TD during hot-pressing. Due to the difference of the yield strength (YS) of dissimilar metals, the volume fraction of each layer after hot-pressing must be distinguished from that before hot-pressing. In order to understand the mechanical properties of LMCs clearly, the thicknesses of Ti layer, Al layer, Mg layer and intermetallic phases layer at different hot-pressing temperatures are measured, as shown in Table 1. It serves to display that the deformations of Mg and Al are similar, while their deformations are greater than that of Ti at various temperatures.

The tensile properties of LMCs hot-pressed at different temperatures along RD are given in Figure 10. Figure 10a shows engineering stress-strain curves of LMCs. And Figure 10b shows variations of YS, the ultimate tensile strength (UTS) and the fracture elongation (FE) of LMCs along RD. It is noticed that UTS of LMCs increases with the temperature increases,

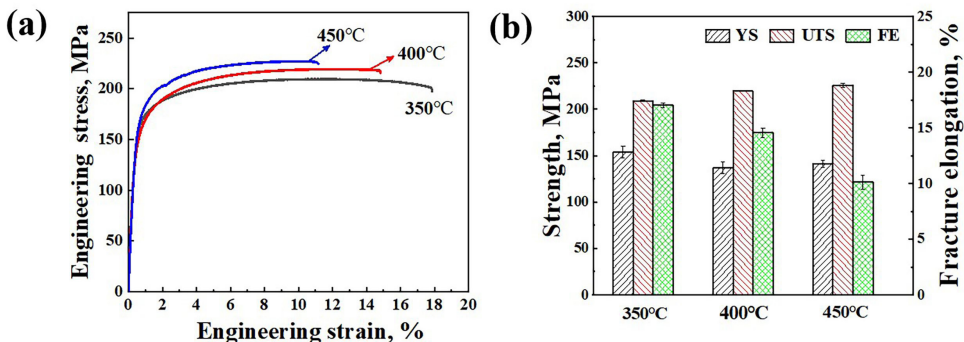


Figure 10. The tensile properties of LMCs hot-pressed at different temperatures along RD: (a) engineering stress-strain curves and (b) variations of YS, UTS and FE.

however, at the expense of FE. The increase of UTS can be attributed to the following aspects. First of all, dislocation strengthening effect is the most significant. Dislocations with three types need to be considered during deformation. With the temperature increases, the deformation of LMCs increases. For example, the deformation of LMCs increases from 19.01% to 28.60% when temperature increases from 350 °C to 450 °C (as shown in Table 1). Which will cause severe shear deformation at the interface. Subsequently greater stress concentrations and more dislocations will generate at the interface. And at high temperature, the cooperative deformation ability of adjacent layers enhances owing to strong interface bonding. Therefore, dislocations easily interact with interface and plug at the interface during plastic deformation. Also, the difference in thermal conductivity between layers causes a local temperature increase. During cooling after deformation, due to different cooling rate, regions with severe thermal stresses are generated, which results in thermal unmatched dislocations at the interface³². All above factors lead to high dislocation density at the interface, so dislocation strengthening theory can explain this strengthening behavior. Moreover, the back stress strengthening at the interface needs to be emphasized. Due to the difference of elastic-plastic properties between component metals and intermetallic compounds, an elastic-plastic deformation stage will be introduced during deformation, which results in the formation of strain gradient. The higher the temperature is, the more severe the shear is at the interface, and the larger strain gradient is. Subsequently, it is necessary to generate some geometrically necessary dislocations (GND) to alleviate the strain gradient. As a result, the back stress enhancement caused by the accumulation of GND leads to higher strength³⁹. At elevated temperature, solid solutions at both Ti/Al and Al/Mg interfaces and intermetallic phases at Al/Mg interface tend to contribute significantly to the increase of strength. Furthermore, with the increasing temperature, high thickness ratio of Ti to LMCs enhances the overall strength of LMCs because of higher strength of Ti than Al and Mg²¹. In addition, the bonding strength of both Ti/Al and Al/Mg interfaces increases when temperature increase from 350°C to 400°C. High bonding strength can delay necking and fracture of poorly ductile metal and improve its work hardening effect. Although the bonding strength of Al/Mg interface declines from 400 °C to 450 °C, the influence of other factors above may be more prominent.

Despite that, the fracture elongation (FE) of LMCs reduces visibly with the increasing temperature, which may be closely related to bonding strength. At 350 °C, debonding occurs easily due to the weak bonding, so more energy is needed for cracks initiation. Also, the weak interface blunts the crack tip and prolongs the crack propagation path. Thus the LMCs possess optimal plasticity at low temperature³¹. Furthermore, intermetallic phases generate at Al/Mg interface. The higher the temperature is, the thicker the intermetallic phases layer is, and the harder it is to coordinate deformation with adjacent sheets. Therefore, it is likely to trigger stress concentration and initiate cracks, so plasticity of LMCs weakens at high temperature.

The fracture macro morphologies of tensile specimens of LMCs at different hot-pressing temperatures are displayed in Figure 11. During tensile, for all specimens, Ti and Al layers are well-bonded, while delamination occurs between Al and Mg layers. As described by the magnified images of Figure 11a, Mg can be observed significantly under Ti/Al layer, which indicates the inhomogeneous deformation between Mg and Ti/Al layers. From the magnified images of Figure 11b, the delamination between Al and Mg as well as the fracture of Mg can be observed clearly. Based on above analysis, during tensile, at low strain, microcracks generate at Al/Mg interface owing to intermetallic compounds, and a large number of microcracks lead to local debonding of Al/Mg interface. With the strain increases, the local debonding extends and interconnects to form delaminations. After that, Mg layer and Ti/Al layer work independently. Subsequently, Mg fractures owing to its poor UTS. While Ti/Al layer deforms unceasingly after the fracture of Mg, because the crack tip is passivated by interface debonding and the renucleation of cracks requires to absorb more energy³⁴. From the partial enlarged views of Figure 11b, the fractured Mg and the well-bonded Ti/Al layer can be observed obviously. Sun et al.⁴¹ also demonstrated that local debonding of interface increased the damage tolerance and the absorbed energy of fracture of LMCs. At high strain levels, Ti layer and Al layer deform cooperatively, necking and breaking occur along the direction of 45° to RD. Ultimately, LMCs rupture. Therefore, the Ti/Al layer plays a key role in the later stages of tensile of LMCs.

Furthermore, curling is noted at Ti/Al layer when hot-pressed at 400 °C and 450 °C, as described in the magnified images of Figure 11b. Which may be attributed to the different thermal expansion coefficients between

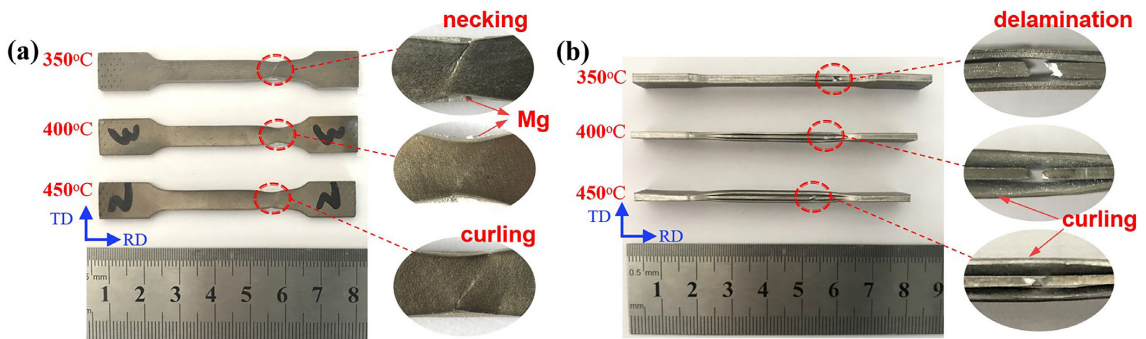


Figure 11. The macro morphologies of tensile specimens of LMCs after rupture at different hot-pressing temperatures: (a) RD-TD surface and (b) RD-ND surface.

Ti and Al. It is thought that the higher the temperature is, the more serious the thermal mismatching is, and the more residual stress is, so the curl is inevitable for Ti/Al layer at elevated temperature²³.

3.5 Mechanical properties of LMCs analyzed by ROM

The strength of LMCs can be calculated by applying ROM¹³:

$$\sigma = \sigma_{Ti}v_{Ti} + \sigma_{Al}v_{Al} + \sigma_{Mg}v_{Mg} \quad (1)$$

$$v_{Ti} + v_{Al} + v_{Mg} = 1 \quad (2)$$

Where σ is the flow stress of LMCs, σ_{Ti} , σ_{Al} and σ_{Mg} are the flow stresses of heat-treated Ti, Al and Mg, respectively, and v_{Ti} , v_{Al} , v_{Mg} are volume fractions of Ti, Al, Mg after hot-pressing, respectively. Relevant dates can be calculate according to Table 1.

In order to understand the tensile properties of LMCs clearly, the component metals are heat-treated at 350 °C, 400 °C and 450 °C, and corresponding engineering stress-strain curves are given in Figure 12. The YS, UTS and FE of monolithic Ti, Al, Mg sheets are summarized in Table 2.

It can be clearly seen from Figure 12 that the ductility of LMCs is lower than any monolithic sheets, while the strength lies between Al sheet and Mg sheet.

LMCs calculated by ROM are regarded as theoretical values. Table 3 exhibits the comparison between the theoretical values and the measured values of LMCs. As shown in Table 3, both theoretical YS and UTS of LMCs decline with the increase of temperature, which is contrary to the results of the measured. Both the measured values of YS and UTS of LMCs are higher than the theoretical, and the gap becomes much more obvious with the increase of temperature.

The variation above may involve many causes and the following five aspects will be discussed emphatically. Firstly, it has been characterized by Figure 5a that Ti/Al interface is rough when hot-pressed at elevated temperature. This roughness may induce some strain, which may directly play on the improvement of strength. Secondly, the interface reaction layer is not considered by ROM. Both solution strengthening and precipitation strengthening should be emphasized. With the increase of temperature, the gap between the theoretical values and the measured values becomes wide because of the thickened solid solution zone and intermetallic phases layer. Thirdly, the deformations of component metals are not considered by ROM. Actually, due to the drastic deformation, both fine grain strengthening and work hardening may generate in monolithic metals. Fourth, according to ROM, the YS of LMCs is calculated based on the YS of monolithic metals. However, the actual yielding happens only when a layer with a high YS yields. In present work, Ti possesses the highest YS, so it is difficult to observe

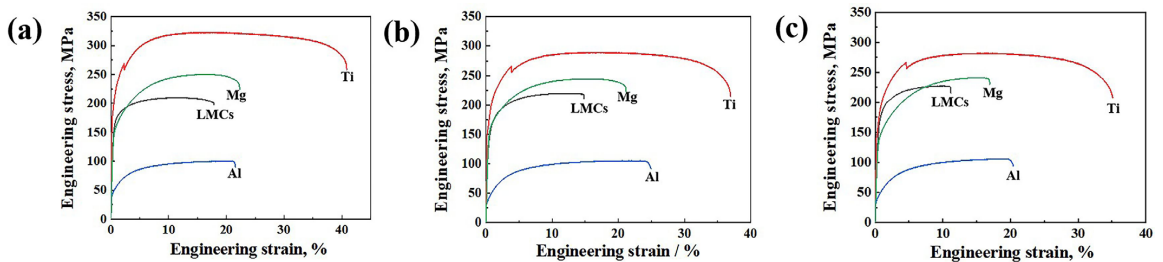


Figure 12. Engineering stress-strain curves of monolithic Ti, Al, Mg sheets and LMCs at the temperature of (a) 350 °C (b) 400 °C and (c) 450 °C.

Table 2. Mechanical properties of monolithic Ti, Al and Mg sheets heat-treated at different temperatures.

Temperature, °C	Test layer	YS, MPa	UTS, MPa	FE, %
350	Ti	180.65±7.06	312.70±14.18	32.25±2.61
	Al	44.35±0.46	103.48±3.28	21.43±2.74
	Mg	158.81±6.88	248.02±5.8	20.73±0.99
400	Ti	163.46±13.35	289.65±15.03	36.88±4.51
	Al	42.61±8.01	102.99±3.52	24.21±1.44
	Mg	157.81±10.02	246.78±2.35	19.07±2.42
450	Ti	167.91±11.85	282.01±14.27	35.06±2.82
	Al	36.86±5.29	102.84±5.01	19.51±0.65
	Mg	137.76±4.89	239.38±1.83	16.29±0.82

Table 3. Comparison of the theoretical values and the measured values of YS and UTS in LMCs at different hot-pressing temperatures.

Temperature, °C	YS, MPa		UTS, MPa	
	Theoretical values	Measured values	Theoretical values	Measured values
350	120.65	153.60	208.76	209.22
400	115.35	136.94	202.11	219.47
450	105.91	141.33	195.73	225.68

the yielding phenomenon of LMCs when monolithic Mg or Al yields. Therefore, deviation between the theoretical values and the measured values is reasonable. Fifth, the constraint effect is expected to be developed. Because of the different elastic-plastic behavior of Ti, Al, Mg, intermetallic phases layer and solid solution layer, the constraint strain will generate when LMCs are subjected to tensile strain⁴². Both the variation of stress state and the formation of GND in different deformation stages will lead to the increase of measured strength.

4. Conclusions

LMCs were fabricated by hot-pressing at 350 °C, 400 °C and 450 °C in present work. The influences of interface morphology, diffusion layer and reaction product, constraint effect on the mechanical properties of LMCs were studied. The detailed conclusions were given as follows:

- (1) With the increase of hot-pressing temperature, the morphologies of Ti/Al interface change from flat to waveform, and intermetallic phases don't form. Whereas, the width of intermetallic phases layer at Mg/Al interface increases significantly with the increasing temperature.
- (2) With the increase of hot-pressing temperature, both bonding strength and hardness of Ti/Al interface increase owing to the thickened diffusion layer. However, the bonding strength of Al/Mg interface doesn't change linearly with the increasing temperature, and the maximum bonding strength is obtained at 400 °C.
- (3) With the increasing temperature, UTS of LMCs increases, however, at the expense of FE. The dislocation strengthening, back stress strengthening, solution strengthening, precipitation strengthening, the delayed necking and the increased Ti content are all contributed to the increase of UTS. The variation of FE is attributed to the influence of interface on crack initiation and propagation.
- (4) Both the measured YS and UTS of the LMCs are higher than that calculated by ROM. It is thought that the strain, solid solution, precipitated phases and stress at the interfaces as well as fine grains, work hardening, inconsistent yielding of monolithic sheets are all conducive to the improvement of the measured strength of LMCs.

5. Acknowledgments

This work was supported by “National Natural Science Foundation of China” (Grants. 51771128 and 51771129), Projects of International Cooperation in Shanxi (Grant no. 201703D421039), Shanxi province science and technology major projects (Grant no.20181101008) and the Program for the Outstanding Innovative Teams of Higher Learning Institutions of Shanxi.

6. References

1. Medeiros RJ, Nóbrega SHS, Aquino EMF. Failure theories on carbon/kevlar hybrid fabric based composite laminate: notch and anisotropy effects. *Mater Res.* 2019;22(3):1-11.
2. Ribeiro AH, Gomez JE, Hale DW, Tonatto MLP, Panzera TH, Thomas C, et al. Evaluation of the stiffening mechanism based on micro-sized particle inclusions in laminated composites. *Mater Res.* 2019;22(4):1-9.
3. Zhang J, Liu S, Wu R, Hou L, Zhang M. Recent developments in high-strength Mg-RE-based alloys: Focusing on Mg-Gd and Mg-Y systems. *Journal of Magnesium and Alloys.* 2018;6(3):277-91.
4. Bridier F, Villechaise P, Mendez J. Analysis of the different slip systems activated by tension in a α/β titanium alloy in relation with local crystallographic orientation. *Acta Mater.* 2005;53(3):555-67.
5. Yang WW, Cao XQ, Wang LF, Chen ZQ, Wang WX, Wang DY. Microstructure and mechanical properties of AA6061/AZ31B/AA6061 composite plates fabricated by vertical explosive welding and subsequent hot rolling. *Mater Res.* 2018;21(6):1-9.
6. Qin L, Wang H, Cui S, Wu Q, Fan M, Yang Z, et al. Characterization and formability of titanium/aluminum laminate composites fabricated by hot pressing. *J Mater Eng Perform.* 2017;26(7):3579-87.
7. Kaibyshev R, Musin F, Lesuer DR, Nieh TG. Superplastic behavior of an Al-Mg alloy at elevated temperatures. *Mater Sci Eng A.* 2003;42:169-77.
8. Zhang X, Yu Y, Liu B, Ren J. Mechanical properties and tensile fracture mechanism investigation of Al/Cu/Ti/Cu/Al laminated composites fabricated by rolling. *J Alloys Compd.* 2019;805:338-45.
9. Qin L, Wang J, Wu Q, Guo X, Tao J. In-situ observation of crack initiation and propagation in Ti/Al composite laminates during tensile test. *J Alloys Compd.* 2017;712:69-75.
10. Fronczek DM, Chulist R, Szulc Z, Wojewoda-Budka J. Growth kinetics of TiAl₃ phase in annealed Al/Ti/Al explosively welded clads. *Mater Lett.* 2017;198:160-3.
11. Tang J, Chen L, Zhao G, Zhang C, Yu J. Study on Al/Mg/Al sheet fabricated by combination of porthole die co-extrusion and subsequent hot rolling. *J Alloys Compd.* 2019;784:727-38.
12. Feng B, Xin Y, Yu H, Hong R, Liu Q. Mechanical behavior of a Mg/Al composite rod containing a soft Mg sleeve and an ultra-hard Al core. *Mater Sci Eng A.* 2016;675:204-11.
13. Du Y, Fan G, Yu T, Hansen N, Geng L, Huang X. Laminated Ti-Al composites: processing, structure and strength. *Mater Sci Eng A.* 2016;673:572-80.
14. Saravanan S, Raghukandan K, Hokamoto K. Improved microstructure and mechanical properties of dissimilar explosive cladding by means of interlayer technique. *Arch Civ Mech Eng.* 2016;16(4):563-8.
15. Chen Z, Wang D, Cao X, Yang W, Wang W. Influence of multi-pass rolling and subsequent annealing on the interface microstructure and mechanical properties of the explosive welding Mg/Al composite plates. *Mater Sci Eng A.* 2018;723:97-108.
16. Zhang XC, Wang CJ, Deng KK, Nie KB, Gan WM, Liang W. Fabrication, microstructure and mechanical properties of the as-rolled ZW31/PMMCs laminate. *Mater Sci Eng A.* 2019;761:138043.
17. Fronczek DM, Chulist LL. Microstructure and kinetics of intermetallic phase growth of three-layered Al1050-AZ31-Al1050 clads prepared by explosive welding combined with subsequent annealing. *Mater Des.* 2017;(130):120-30.
18. Assari AH, Eghbali B. Interfacial layers evolution during annealing in Ti-Al multi-laminated composite processed using hot press and roll bonding. *Met Mater Int.* 2016;22(5):915-23.
19. Fan M, Domblesky J, Jin K, Qin L, Cui S, Guo X, et al. Effect of original layer thicknesses on the interface bonding and mechanical properties of Ti Al laminate composites. *Mater Des.* 2016;99:535-42.
20. Sun Y, Wan ZP, Hu LX, Wu BH, Deng TQ. Characterization on solid phase diffusion reaction behavior and diffusion reaction kinetic of Ti/Al. *Rare Met Mater Eng.* 2017;46(8):2080-6.

21. Yu H, Tieu AK, Li H, Godbole A, Kong C. Annealing effect on microstructure and mechanical properties of Al/Ti/Al laminate sheets. *Mater Sci Eng A*. 2016;660:195-204.
22. Nie H, Hao X, Chen H, Kang X, Wang T, Mi Y, et al. Effect of twins and dynamic recrystallization on the microstructures and mechanical properties of Ti/Al/Mg laminates. *Mater Des*. 2019;181:107948.
23. Kaya İ, Cora ÖN, Acar D, Koç M. On the formability of ultrasonic additive manufactured Al-Ti laminated composites. *Metall Mater Trans, A Phys Metall Mater Sci*. 2018;49(10):5051-64.
24. Wang T, Nie H, Mi Y, Hao X, Yang F, Chi C, et al. Microstructures and mechanical properties of Ti/Al/Mg/Al/Ti laminates with various rolling reductions. *J Mater Res*. 2018;34(2):344-53.
25. Liu CY, Wang Q, Jia YZ, Jing R, Zhang B, Ma MZ, et al. Microstructures and mechanical properties of Mg/Mg and Mg/Al/Mg laminated composites prepared via warm roll bonding. *Mater Sci Eng A*. 2012;556:1-8.
26. Nie H, Chi C, Chen H, Li X, Liang W. Microstructure evolution of Al/Mg/Al laminates in deep drawing process. *J Mater Res Technol*. 2019;8(6):5325-35.
27. Choi DH, Ahn BW, Lee CY, Yeon YM, Song K, Jung SB. Formation of intermetallic compounds in Al and Mg alloy interface during friction stir spot welding. *Intermetallics*. 2011;19:125-30.
28. Ma M, Meng X, Liu WC. Microstructure and mechanical properties of Ti/Al/Ti laminated composites prepared by hot rolling. *J Mater Eng Perform*. 2017;26(7):3569-78.
29. Lyu S, Sun Y, Li G, Xiao W, Ma C. Effect of layer sequence on the mechanical properties of Ti/TiAl laminates. *Mater Des*. 2018;143:160-8.
30. Sauvage X, Dinda GP, Wilde G. Non-equilibrium intermixing and phase transformation in severely deformed Al/Ni multilayers. *Scr Mater*. 2007;56(3):181-4.
31. Xia HB, Wang SG, Ben HF. Microstructure and mechanical properties of Ti/Al explosive cladding. *Mater Des*. 2014;56:1014-9.
32. Du Y, Fan GH, Yu T, Hansen N, Geng L, Huang X. Effects of interface roughness on the annealing behaviour of laminated Ti-Al composite deformed by hot rolling. *Mater Sci Eng A*. 2015;89:7.
33. Huang M, Xu C, Fan G, Maawad E, Gan W, Geng L, et al. Role of layered structure in ductility improvement of layered Ti-Al metal composite. *Acta Mater*. 2018;153:235-49.
34. Launey ME, Ritchie RO. On the fracture toughness of advanced materials. *Adv Mater*. 2009;21(20):2103-10.
35. Bouaziz O, Sauvage X, Barcelo D. Steel-magnesium composite wire obtained by repeated co-extrusion. *Mater Sci Forum*. 2010;654-656:1263-6.
36. Zhang XP, Tan MJ, Yang TH, Xu XJ, Wang JT. Bonding strength of Al/Mg/Al alloy tri-metallic laminates fabricated by hot rolling. *Bull Mater Sci*. 2011;34(4):805-10.
37. Chang HW, Zhang MX, Atrens A, Huang H. Nanomechanical properties of Mg-Al intermetallic compounds produced by packed powder diffusion coating (PPDC) on the surface of AZ91E. *J Alloys Compd*. 2014;587:527-32.
38. Yang H, Guo X, Wu G, Wang S, Ding W. Continuous intermetallic compounds coatings on AZ91D Mg alloy fabricated by diffusion reaction of Mg-Al couples. *Surf Coat Tech*. 2011;205(8-9):2907-13.
39. Chen Y, Nie J, Wang F, Yang H, Wu C, Liu X. Revealing hetero-deformation induced (HDI) stress strengthening effect in laminated Al-(TiB₂+TiC)p/6063 composites prepared by accumulative roll bonding. *J Alloys Compd*. 2020;815:1-8.
40. Mi Y, Nie H, Wang T, Li X, Hao X, Liang W. Effect of anisotropy on microstructures and mechanical properties of rolled Ti/Al/Mg/Al/Ti laminates. *J Mater Eng Perform*. 2019;28(7):4143-51.
41. Sun Y, Chen J, Ma F, Ameyama K, Xiao W, Ma C. Tensile and flexural properties of multilayered metal/intermetallics composites. *Mater Charact*. 2015;102:165-72.
42. Wu H, Fan G, Huang M, Geng L, Cui X, Xie H. Deformation behavior of brittle/ductile multilayered composites under interface constraint effect. *Int J Plast*. 2017;89:96-109.